A flexible model of the microwave sky for CCAT-prime and other future CMB survey instruments

Maude Charmetant & Jens Erler

February 2, 2023

Contents

1 Overview

We provide a high resolution (native pixel size $\approx 0.86'$) model of the microwave sky that should allow for the creation of realistic mock data sets in the frequency range of 27GHz $< \nu <$ 860 GHz. The individual components of the sky model can be divided into three groups, namely Galactic emission, extragalactic emission, and noise.

We simulate Galactic synchrotron, free–free, thermal dust, and AME using the python sky model (PySM, Thorne et al. 2017), which uses the most recent Galactic foreground maps

obtained by the Planck Collaboration (2016). Extragalactic emission, i.e. the CMB, CIB, radio point sources, and the SZ signals of clusters, are obtained from numerical simulations by Sehgal et al. (2010), the Simons Observatory Collaboration (Ade et al. 2019), and Stein et al. (WebSky, 2020). While the simulations performed by Sehgal et al. (2010) are based on n-body physics, Stein et al. (2020) use a fast and novel peak patch simulation technique. The simulations provided by the Simons Observatory Collaboration (Ade et al. 2019) present a re-calibrated version of the ones presented by Sehgal et al. (2010) and match current observational constraints obtained by *Planck*. The results of these simulations are provided by the respective groups as flux maps at a set of given frequencies. We use interpolation techniques to extrapolate each component to the frequency range that is relevant for CCAT-prime. In addition to these astrophysical signals, the sky model provides functions that add either white noise or a realistic atmospheric noise, computed using the model presented by Choi et al. (2019), to the simulated maps.

The individual components of the sky model are described in more detail below. Table 1 gives an overview of the components of the sky model and their properties and limitations. The results of the sky model are stored at Healpy all-sky maps. In addition to the functions that simulate the sky, we provide tools to extract small fields from the all-sky maps and draw random, uniformly distributed sky positions for the purpose of covariance estimation. The sky model can be downloaded from `https://github.com/MaudeCharmetant/CCATp_sky_model`. The all-sky maps required to run the sky model are available on `https://uni-bonn.sciebo.de/s/tyFVBUdjJ4BqDMB`

2 Simulations/templates

2.1 The CITA WebSky extragalactic CMB mocks

The WebSky simulations provide HEALPix all-sky maps of the extragalactic sky at $N_{\rm side} = 4096$. The provided components include the CIB, tSZ, kSZ, and the lensed/unlensed CMB. Additional background of extragalactic radio point sources is being prepared and will be available soon. The large-scale structure was obtained through a peak-patch and 2LPT simulation with 12288^3 particles and a box size of $15.4\,h^{-1}$ Gpc. Technical remarks on the simulations algorithm are presented in Stein et al. (2019). The authors assume a flat ΛCDM cosmology with $h = 0.68$, $\Omega_{\rm cdm} = 0.261$, $\Omega_b = 0.049$, $\Omega_\Lambda = 0.69$, $n_s = 0.965$, and $\sigma_8 = 0.81$. The component maps are either provided in units of MJy/sr (CIB), $\mu K_{\rm CMB}$ (kSZ, CMB), or unitless Compton-y (tSZ). While the CMB and SZ signals are frequency independent to first order, the CIB intensity is provided at frequencies ranging from 93 up to 857 GHz, covering the frequencies that were observed by the *Planck* HFI instrument. A detailed description of the WebSky simulations is provided by Stein et al. (2020) and the data can be downloaded from `https://mocks.cita.utoronto.ca/index.php/WebSky_Extragalactic_CMB_Mocks`. We make use of the most recent version of the provided file up until the 27$^{\rm th}$ of January 2020.

component	template	effective resolution	limitations
		diffuse high-z backgrounds	
CMB	SO, WebSky, Sehgal, or any C_ℓ	$N_{\rm side} = 4096$, $0.86'$	–
CIB	SO, WebSky, or Sehgal	$N_{\rm side} = 4096$, $0.86'$	extrapolation for $\nu > 350\,$GHz necessary for SO and Sehgal
		Galactic foregrounds	
synchrotron	PySM, model 's1'	$N_{\rm side} = 512$, $6.9'$	low spatial resolution
free–free	PySM, model 'f1'	$N_{\rm side} = 512$, $6.9'$	low spatial resolution
thermal dust	PySM, model 'd1'	$N_{\rm side} = 512$, $6.9'$	low spatial resolution
AME	PySM, model 'a1'	$N_{\rm side} = 512$, $6.9'$	low spatial resolution
		point sources	
radio PS	SO & Sehgal	$N_{\rm side} = 4096$, $0.86'$	high-ν extrapolation for Sehgal lin interp. in $30 < \nu < 350\,$GHz for SO not available for Websky
		galaxy clusters	
tSZ	SO, WebSky, Sehgal	$N_{\rm side} = 4096$, $0.86'$	no working halo catalogs no rel. corr. applicable
kSZ	SO, WebSky, Sehgal	$N_{\rm side} = 4096$, $0.86'$	no working halo catalogs
		Noise	
white noise	given sensitivities	arbitrary	–
atmosheric noise	Choi et al. (2019)	arbitrary	only at SO and CCAT-p freq. no tools to simulate characteristic "stripy" survey noise

Table 1 – Components of the skymodel.

2.2 The Sehgal et al. (2010) simulations

A high-resolution model of the microwave sky is provided by Sehgal et al. (2010) at frequencies ranging from 30 to 350 GHz. The sky model is available as a set of HEALPix all-sky maps with $N_{\rm side} = 8192$ and units of Jy/sr. The components of the model include the lensed/unlensed CMB, the tSZ, the kSZ, radio galaxies, infrared galaxies (CIB), and Galactic dust. The large-scale structure, from which these maps were derived, was obtained from a tree-particle-mesh simulation that was run on a $1\,h^{-1}$ Gpc box containing 1024^3 particles, while assuming a flat ΛCDM cosmology with $h = 0.71$, $\Omega_{\rm cdm} = 0.22$, $\Omega_b = 0.049$, $\Omega_\Lambda = 0.736$, $n_s = 0.96$, and $\sigma_8 = 0.80$ that is consistent with the WMAP5 results (Komatsu et al. 2009). The all-sky maps are built from eight identical octants of the full sky. A noteworthy feature of these simulations is the correlation of radio and infrared galaxies with the galaxy cluster population. The Galactic dust emission is simulated using oversampled model fit IRAS and COBE data and was dropped by us in favor of more recent *Planck* templates that also include other relevant Galactic foregrounds. The Sehgal et al. (2010) sky model can be downloaded from `https://lambda.gsfc.nasa.gov/simulation/tb_sim_ov.cfm`.

2.3 The Simons Observatory (SO) sky model

A modified version of the sky model presented by Sehgal et al. (2010) was used by the SO collaboration for the preparation of their science case (Ade et al. 2019). The SO sky model is provided as a series of HEALPix all-sky maps at $N_{\rm side} = 4096$ at frequencies ranging from 27 to 353 GHz. All maps, except the tSZ y- and lensing convergence maps, come in frequency-independent units of thermodynamic CMB temperature, $\mu K_{\rm CMB}$. To ensure agreement with the most recent ACT, SPT, and *Planck* measurements, the SO sky model modifies the Sehgal et al. (2010) simulations in several ways. Both the tSZ and CIB maps are scaled with a factor of 0.75, while the CMB and kSZ are left untouched. Radio point sources with flux densities greater than 7 mJy at 148 GHz were masked in order to mimic the effect of a mask constructed from a source catalog. The Galactic foreground maps were replaced with more recent *Planck*-based ones obtained through the PySM Thorne et al. (2017) that were left at their native resolution of $\sim 10'$. All maps were downgraded from $N_{\rm side} = 8192$ to $N_{\rm side} = 4096$ using the HEALPix alter_alm() routine. The frequency range of the Sehgal et al. (2010) was extended through pixel-by-pixel interpolation of the flux as a function of frequency using a piecewise linear spline in log-log space. The SO sky model can be downloaded from https://lambda.gsfc.nasa.gov/simulation/tb_sim_ov.cfm

3 How to use the skymodel

The skymodel is developed on GitHub and can be installed by cloning the source repository and running the *setup.py* file:

```
git clone https://github.com/MaudeCharmetant/skymodel.git
cd skymodel
python setup.py install
```

Before the installation is finished by executing the final line, the path to the template all-sky maps should be provided. The path is defined through the variable *data_path* in the 12$^{\rm th}$ line of the file *skymodel.py*. The maps can be downloaded from https://uni-bonn.sciebo.de/s/zgPsb7qvXTnNsr0/authenticate with the password:pw4referee.

Once installed, the sky model can be imported with

```
import skymodel as sky
```

and is called via a central function *skymodel()*, which calls all individual components and combines them into a single output map.

```
def skymodel(freq, sensitivity = None, components = 'all',
    red_noise = False, cl_file = None, lensed = True, out_file = None,
    nside_out = 4096, lmax = None, beam_FWHM = None, template = 'WebSky',
    unit = 'cmb'):
```

In principle, the skymodel will return a map at any given frequency. However, in practice, we strongly recommend staying within the range of 27GHz $< \nu <$ 860 GHz and note that

the Sehgal et al. (2010) and SO sky models rely on extrapolation for $\nu > 350\,\mathrm{GHz}$. The components of the sky that are to be used can be specified as a list of strings. Our sky model allows the user to define the Healpy N_{side} value and the units of the output map. By default, maps will be returned at the native N_{side} of the templates, which is 4096. The default unit is thermodynamic temperature K_{CMB}, but can be changed to brightness temperature K_{RJ} or surface brightness MJy/sr. If desired, the output map can be smoothed with a Gaussian of a given FWHM. Details on the individual parameters of all functions are provided in the function docstrings, which have been prepared with great care.

4 Individual Components

4.1 Galactic foregrounds

```
def simulate_gal_foregrounds(freq, components = 'all', nside_out = 4096,
    lmax = None, beam_FWHM = None, intrinsic_FWHM = 10, unit = 'cmb'):
```

Maps of Galactic synchrotron, free–free, spinning dust, and thermal dust emission are obtained through the Python sky model (PySM, Thorne et al. 2017). The PySM uses the most recent Galactic foreground maps published by the Planck Collaboration (2016) that were built from the full 2015 *Planck* data together with auxiliary data from the WMAP satellite and the 408 MHz all-sky survey by Haslam et al. (1981, 1982), which has been reprocessed by Remazeilles et al. (2015). These foreground templates were obtained with the COMMANDER algorithm and are provided at a native HEALPix resolution of $N_{\mathrm{side}} = 256$. The PySM upgrades these maps to $N_{\mathrm{side}} = 512$ and adds small-scale fluctuations to the maps by extrapolating their power spectra and generating random features according to it, similar to the approach presented by Miville-Deschênes et al. (2007). We use the basic spectral model for each component (i.e. "s1", "f1", "d1", and "a1"; see Fig. 1) to compute component maps at a given frequency. These maps are then further upgraded to higher N_{side} and smoothed with a narrow Gaussian (FWHM = 10′) in order to mitigate pixelation artifacts (see Fig. 2).

4.2 The cosmic infrared background (CIB)

```
def simulate_cib(freq, nside_out = 4096, lmax = None, beam_FWHM = None,
    template = 'WebSky', unit = 'cmb'):
```

We model the expected contribution from the CIB by adopting the synthetic all-sky CIB maps provided by Sehgal et al. (2010), WebSky, and the SO. The maps from all these simulations are provided at specific frequencies. We extrapolate the CIB model to arbitrary frequencies by fitting each pixel with a modified blackbody in order to derive three all-sky parameter value maps for the variables T and β. The flux density in each pixel is then given by

$$I_{\mathrm{CIB}}(\nu) = I(\nu = \nu_0) \left(\frac{\nu}{\nu_0}\right)^{\beta+3} \frac{\exp(h\nu_0/(k_{\mathrm{B}}T)) - 1}{\exp(h\nu/(k_{\mathrm{B}}T)) - 1}, \tag{1}$$

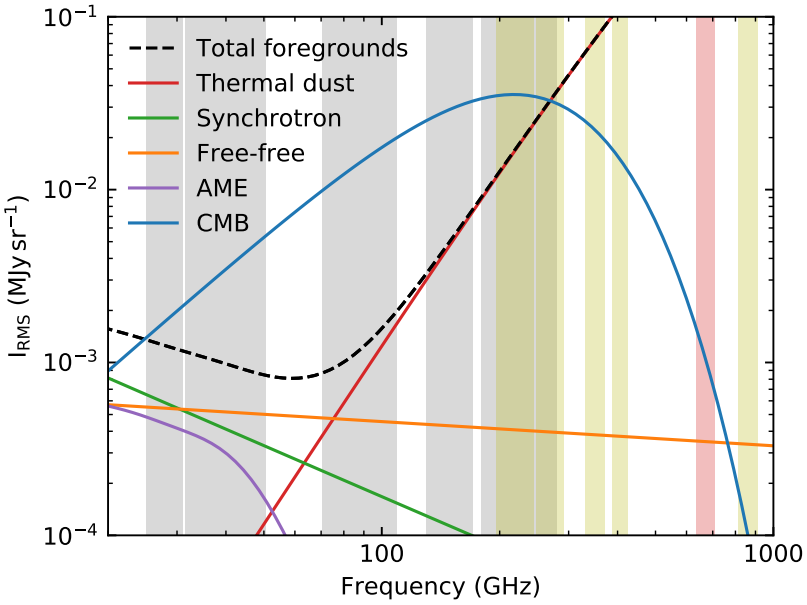

Figure 1 – Spectra of the Galactic foregrounds used in the CCAT-prime sky model presented in Section 4.1, generated using the PySM (Thorne et al. 2017). The colored curves show the standard deviation of the individual components on a scale of 7 arcmin, defined by the HEALPix resolution of the all-sky templates of $N_{\rm side} = 512$. The dashed black line gives the sum of all Galactic foregrounds, while the solid blue line shows the spectrum of the primary CMB temperature anisotropies. The grey and yellow bands indicate the proposed frequency channels for Adv. ACT and a five-channel version of CCAT-prime, respectively. The red band shows the location of a potential 670 GHz CCAT-prime channel that would be permitted by a corresponding atmospheric window.

where $\nu_0 = 353\,\mathrm{GHz}$ (SO & WebSky) or $\nu_0 = 350\,\mathrm{GHz}$ (Sehgal). Finally, the obtained maps are upgraded to higher $N_{\rm side}$ and smoothed with a Gaussian if necessary. Note that the CIB maps used by the SO sky model have been obtained by re-scaling the CIB maps presented by Sehgal et al. (2010) by a factor of 0.75 at all scales (Ade et al. 2019) in order to match the most recent CIB observations.

4.3 Radio point sources

```
def simulate_radio_ps(freq, nside_out = 4096, lmax = None,
    beam_FWHM = None, template = 'WebSky', unit = 'cmb'):
```

A radio point source background is provided by Sehgal et al. (2010) and the related SO sky model. The WebSky simulations currently do not provide radio point sources but will add them in a future release. Due to the complicated spectra that we find for the sources in the SO simulations, which are caused by the ringing artifacts introduced by processing the maps with alter_alm(), we choose two different interpolation techniques. We confine the frequency range for interpolation of the SO maps to the one provided by the input maps, i.e. $27\,\mathrm{GHz} < \nu < 353\,\mathrm{GHz}$. The interpolation itself is performed pixel by pixel through linear interpolation of the original data. The sources seen in the simulations provided by Sehgal et al. (2010) show

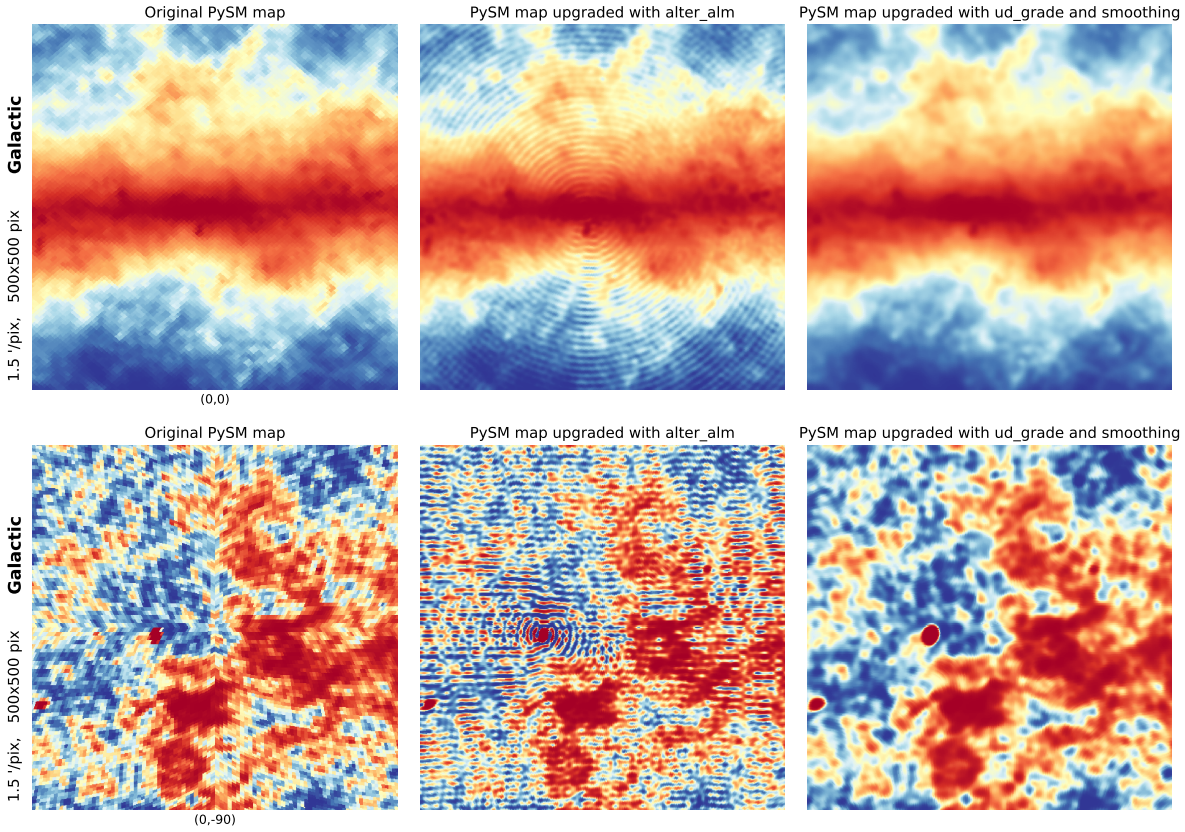

Figure 2 – Illustration of the processing of the Galactic foreground maps produced with the PySM. All panels are gnomic $12.5° \times 12.5°$ projections and show the sum of all Galactic foreground components at a frequency of 353 GHz. The images in the upper row are centered on the Galactic center, while the panels in the lower row show the region around the Galactic south pole. All images are shown in histogram-equalized colors. The two left-hand panels show the oversampled, but otherwise unmodified, original PySM images, which feature pixelation artifacts due to their native pixel size of 6.9′ ($N_{\rm side} = 512$). The center panels where upgraded to a higher $N_{\rm side}$ of 2048 in spherical harmonic space using the alter_alm() function before being projected. This procedure was applied e.g. for the creation of the SO sky model maps from the original Sehgal et al. (2010) maps but produces strong ringing artifacts around point sources. The right-hand panels were obtained by first changing the $N_{\rm side}$ of the original PySM maps to 2048 by simple oversampling using ud_grade(), followed by smoothing with a Gaussian kernel of a width that is comparable to the original pixel size of the PySM maps (FWHM = 10′). This technique removes the pixelation artifacts without adding ringing noise while only marginally lowering the spatial resolution of the maps and was thus chosen to upgrade Galactic foreground maps to higher $N_{\rm side}$.

mostly power-law-shaped spectra, some of which display curvature at higher frequencies. We allow for extrapolation of these spectra to high frequencies > 353 GHz through pixel-by-pixel fitting of the spectra with a curved power-law SED

$$I(\nu) = I(\nu = 30\,\mathrm{GHz}) \left(\frac{\nu}{30\,\mathrm{GHz}}\right)^{\alpha} \exp\left(-\frac{\nu}{\nu_{\mathrm{crit.}}}\right), \tag{2}$$

where α is the spectral index and $\nu_{\mathrm{crit.}}$ is the frequency at which the spectrum begins to show curvature. In units of brightness temperature, α is found to have typical values around −0.8.

4.4 The cosmic microwave background (CMB)

```
def simulate_cmb(freq, cl_file = None, lensed = True, nside_out = 4096,
    lmax = None, beam_FWHM = None, template = 'WebSky', unit = 'cmb'):
```

Our function for generating CMB maps, *simulate_CMB()*, allows choosing from three simulations-based templates (WebSky, SO sky model, and Sehgal et al. (2010)) or alternatively create a random CMB realization from a given CMB power spectrum. Based on those templates, the code will return a CMB map at a given frequency and in the unit of choice. By default, the code will use the lensed WebSky template and no smoothing will be applied.

WebSky : Offers us two files containing random realizations of the primary T/Q/U $a_{\ell m}$ coefficients, one being unlensed and one being lensed. The lensed one has been obtained using the unlensed $a_{\ell m}$ file and the CMB lensing convergence from $0 < z < 1100$ in the Born approximation. Those $a_{\ell m}$ are given for the cosmology defined earlier. Their units are $\mu K_{\rm CMB}$. Those $a_{\ell m}$ are transformed into two maps, a lensed CMB and an unlensed CMB. Our code only reads the lensed map when lensed=True and the unlensed one when lensed=False.

SO : Offers us only a lensed CMB temperature anisotropy map in units of $\mu K_{\rm CMB}$. This lensed CMB map is coming from Ferraro and Hill (2018) and is generated by applying the LensPix code to an unlensed CMB map generated at $N_{\rm side} = 4096$ from a power spectrum computed with CAMB going up to $l = 10\,000$ and a deflection field from the $\kappa_{\rm CMB}$ in Sehgal et al. (2010) (see Ade et al. 2019).

Sehgal : Offers us lensed and unlensed maps of the CMB surface brightness (Jy/sr) at frequencies of 30, 90, 148, 219, 277 and 350 GHz. We create a single, frequency-independent template from the 30 GHz map by multiplying it by the following factor to convert the map into frequency-independent units of $\mu K_{\rm CMB}$.

$$10^{-20}\,\frac{(hc)^2}{2k_B^3 T_{CMB}^2}\,\frac{(e^x-1)^2}{x^4 e^x} \quad \text{with} \quad x_\nu = \frac{h\,\nu}{k_{\rm B}\,T_{\rm CMB}} \quad \text{and} \quad \nu = 30\,\text{GHz} \tag{3}$$

Custom C_ℓ file : As an alternative to the CMB maps that are provided as part of the numerical templates discussed previously, *simulate_CMB()* allows the creation of random realizations of a given CMB power spectrum. Such randomized maps can be useful e.g. for all-sky null tests. By default, the optional parameter *cl_file* expects an ASCII file, whose first two columns are ℓ (starting at 2) and C_ℓ. Such power spectra can be generated e.g. with CAMB.

4.5 Thermal Sunyaev-Zeldovich (tSZ) effect

```
def simulate_tSZ(freq, nside_out = 4096, lmax = None, beam_FWHM = None,
    template = 'WebSky', unit = 'cmb'):
```

Maps of the all-sky tSZ effect are generated with the *simulate_tSZ()* function. The function uses one of the three available templates (WebSky, SO, and Sehgal), all of which simulate the tSZ effect in its non-relativistic limit. While the WebSky and SO sky models provide all-sky Compton-y maps, Sehgal et al. (2010) provide maps of the frequency-dependent tSZ decrement/increment. Analogous to our treatment of the CMB, we obtain a frequency-independent Compton-y map from the Sehgal 30 GHz tSZ all-sky map assuming the non-relativistic spectrum of the tSZ effect:

$$f(\nu, T_\mathrm{e} = 0\,\mathrm{keV}) = x_\nu \frac{e^{x_\nu}+1}{e^{x_\nu}-1} - 4 \quad \text{with} \quad x_\nu = \frac{h\,\nu}{k_\mathrm{B}\,T_\mathrm{CMB}} \quad \text{and} \quad \nu = 30\,\mathrm{GHz} \tag{4}$$

Note that the tSZ map used by the SO sky model has been obtained by re-scaling the tSZ maps presented by Sehgal et al. (2010) by a factor of 0.75 at all scales (Ade et al. 2019) in order to match the most recent measurements by Planck, ACT, and SPT (Planck Collaboration et al. 2014d, 2016h; Singh et al. 2016; George et al. 2015)

4.6 Kinetic Sunyaev-Zeldovich (kSZ) effect

```
def simulate_kSZ(freq, nside_out = 4096, lmax = None, beam_FWHM = None,
   template = 'WebSky', unit = 'cmb'):
```

The function *simulate_kSZ()* allows generating all-sky maps of the kSZ effect, which are either based on the WebSky, the SO, or the Sehgal et al. (2010) sky model. While the WebSky and SO all-sky kSZ maps have native units of μK_CMB and are thus frequency-independent, Sehgal et al. (2010) provide their kSZ maps at a specific set of frequencies in units of Jy/sr. We adopt their 30 GHz map and convert it to units of μK_CMB by multiplying the map with

$$10^{-20}\,\frac{(hc)^2}{2k_B^3 T_{CMB}^2}\,\frac{x^4 e^x}{(e^x-1)^2} \quad \text{with} \quad x_\nu = \frac{h\,\nu}{k_\mathrm{B}\,T_\mathrm{CMB}} \quad \text{and} \quad \nu = 30\,\mathrm{GHz}. \tag{5}$$

Note that the WebSky kSZ map is split into two components, the contribution of collapsed halos and field ($z < 4.5$) and the "patchy" contribution of gas during reionization ($z > 5.5$). The sky model presented here only makes use of the first "halo" component. More information on the differences can be found in Stein et al. (2020).

4.7 All-sky white noise maps

```
def simulate_white_noise(freq, noise_level, nside_out = 4096,
   unit_noise = 1, arcmin = True, unit = 'cmb'):
```

All-sky maps containing white noise can be obtained using the function *simulate_white_noise()*. This function takes a given noise level in units of μK_CMB-arcmin and converts it to a pixel-size-dependent standard deviation to generate Gaussian white noise. The pixel size is computed as a function of the Healpy N_side parameter value. If desired, the all-sky white noise map is then converted to different units using the provided frequency.

4.8 CCAT-prime atmospheric model

```
def simulate_atmosphere(freq, nside_out = 4096, lmax = None,
    beam_FWHM = None, unit = 'cmb', no_white = False):
```

In addition to white noise, the sky model presented here offers the possibility to include the realistic white + red atmospheric noise model that was presented by the SO Collaboration (Ade et al. 2019) and adopted for CCAT-prime by Choi et al. (2019):

$$N_\ell = N_{\rm red}\left(\frac{\ell}{\ell_{\rm knee}}\right)^{\alpha_{\rm knee}} + n_{\rm white}, \tag{6}$$

where $\ell_{\rm knee} = 1000$ and $\alpha_{\rm knee} = -3.5$. The values for $N_{\rm red}$ and $N_{\rm white}$ for the SO and for CCAT-prime are included in the sky model. Note that the values used here were obtained through private communication with Steve Choi and are more recent than the numbers given in the respective publications. The atmospheric noise model can only be computed at a valid SO frequency (27, 39, 93, 145, 225 & 279 GHz) or CCAT-prime frequency (225, 280, 350, 410 & 850 GHz) and takes the form of a series of power spectra, as defined by equation (6) and shown in Fig. 3. The function *simulate_atmosphere()* creates all-sky realizations of the sky based on these given spectra using the *synfast()* function of Healpy. Note that the resulting maps are generated using isotropic Gaussian random fields, i.e. the noise will be "patchy" rather than "stripy" (see Fig. 4).

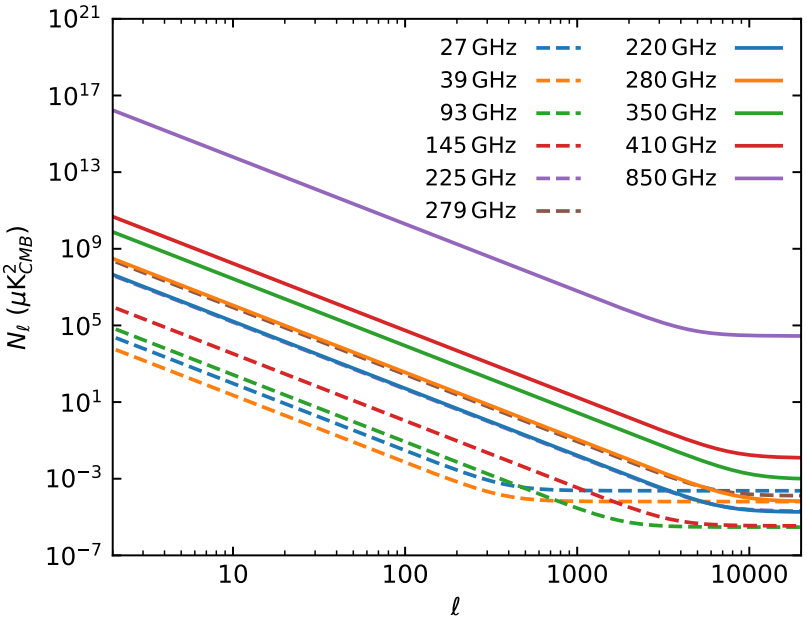

Figure 3 – SO (dashed lines) and CCAT-p (solid lines) atmospheric noise spectra based on the noise model presented by Ade et al. (2019) and adopted by Choi et al. (2019).

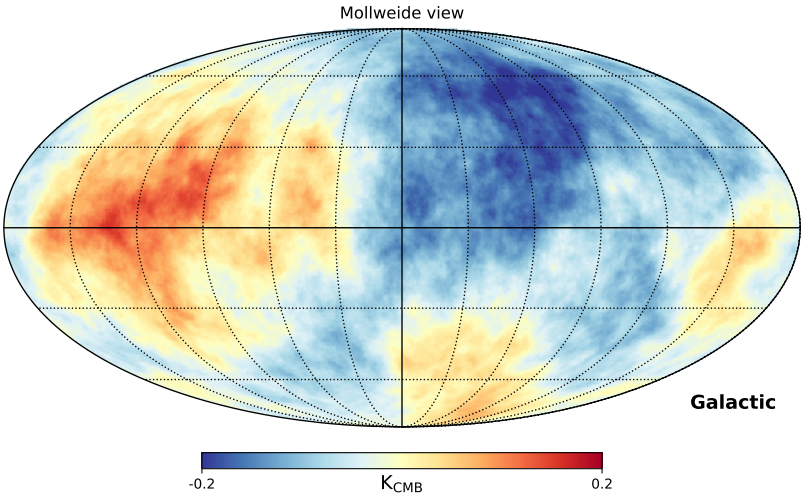

Figure 4 – Random all-sky realization of the survey noise expected for the CCAT-prime 350 GHz channel.

4.9 Survey masks

```
1 def return_mask(survey, nside_out = 256, coord = 'G'):
```

In addition to the maps of astrophysical emission and noise, we provide a series of masks that either correspond to the sky area surveyed by current or future surveys, or to masks that exclude the Galactic plane for studies using all-sky data like the one delivered by *Planck*. All masks are stored at $N_{\rm side} = 256$ and can be accessed and upgraded to a different $N_{\rm side}$ using the *return_mask()* function. An overview of the available masks is given in Fig. 5.

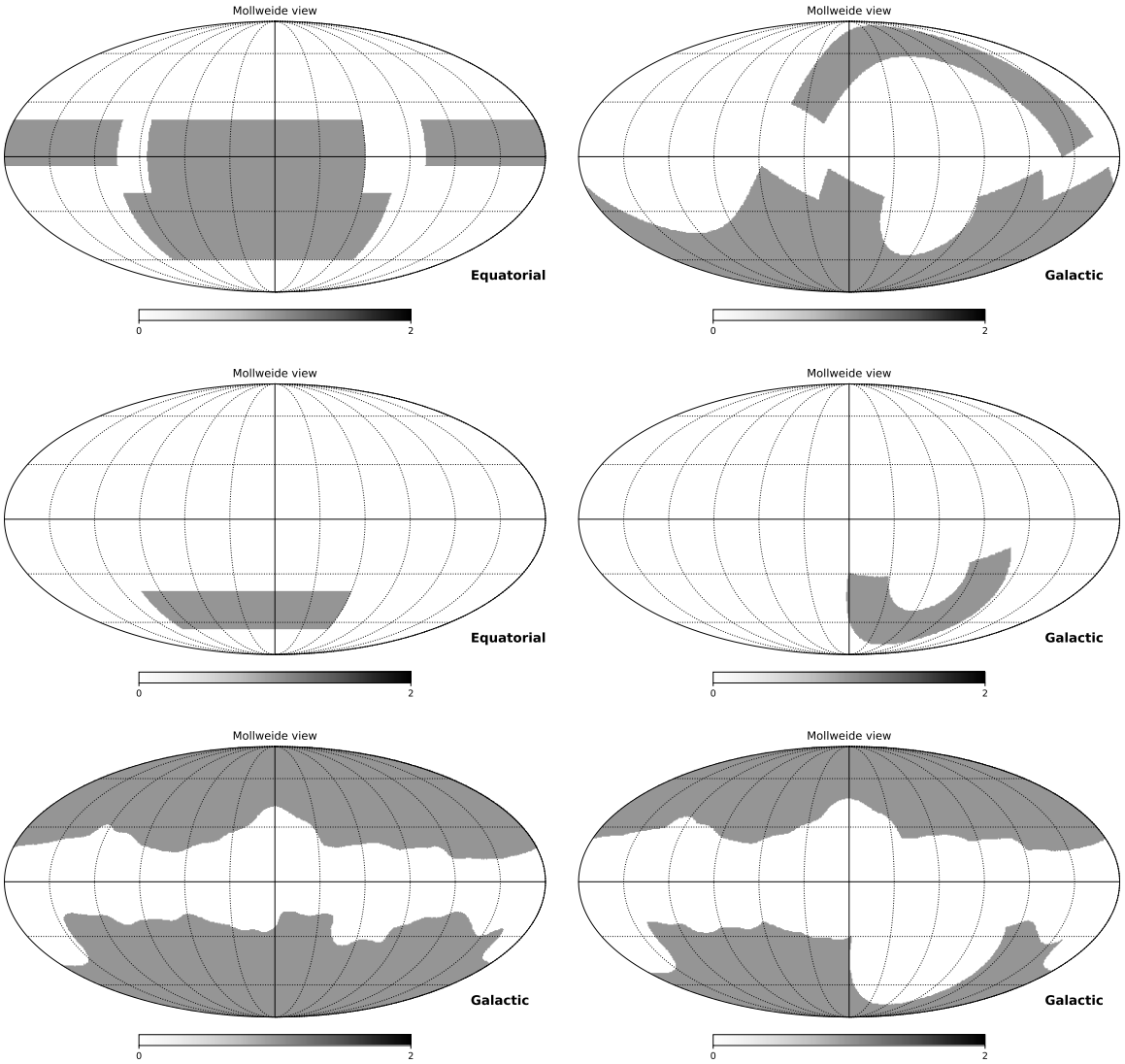

Figure 5 – All-sky masks that are part of the sky model. The two upper panels show the survey mask for the Adv. ACT survey covering an area of $\sim$ 15 000 sq. deg. ($f_{\rm sky} \approx 0.4$). The SO and CCAT-prime wide-area surveys are proposed to observe the same field. The two panels in the middle row show equivalent survey masks for the 2500 sq. deg. SPT-SZ survey ($f_{\rm sky} \approx 0.06$). The two bottom panels show Galactic foreground masks derived from *Planck* data. While the one shown in the left-hand panel ($f_{\rm sky} \approx 0.6$) was used by Erler et al. (2018), the mask shown in the right-hand panel ($f_{\rm sky} \approx 0.45$) was used for more recent CCAT-prime forecasts and excludes the part of the sky that was not observed by the NVSS.

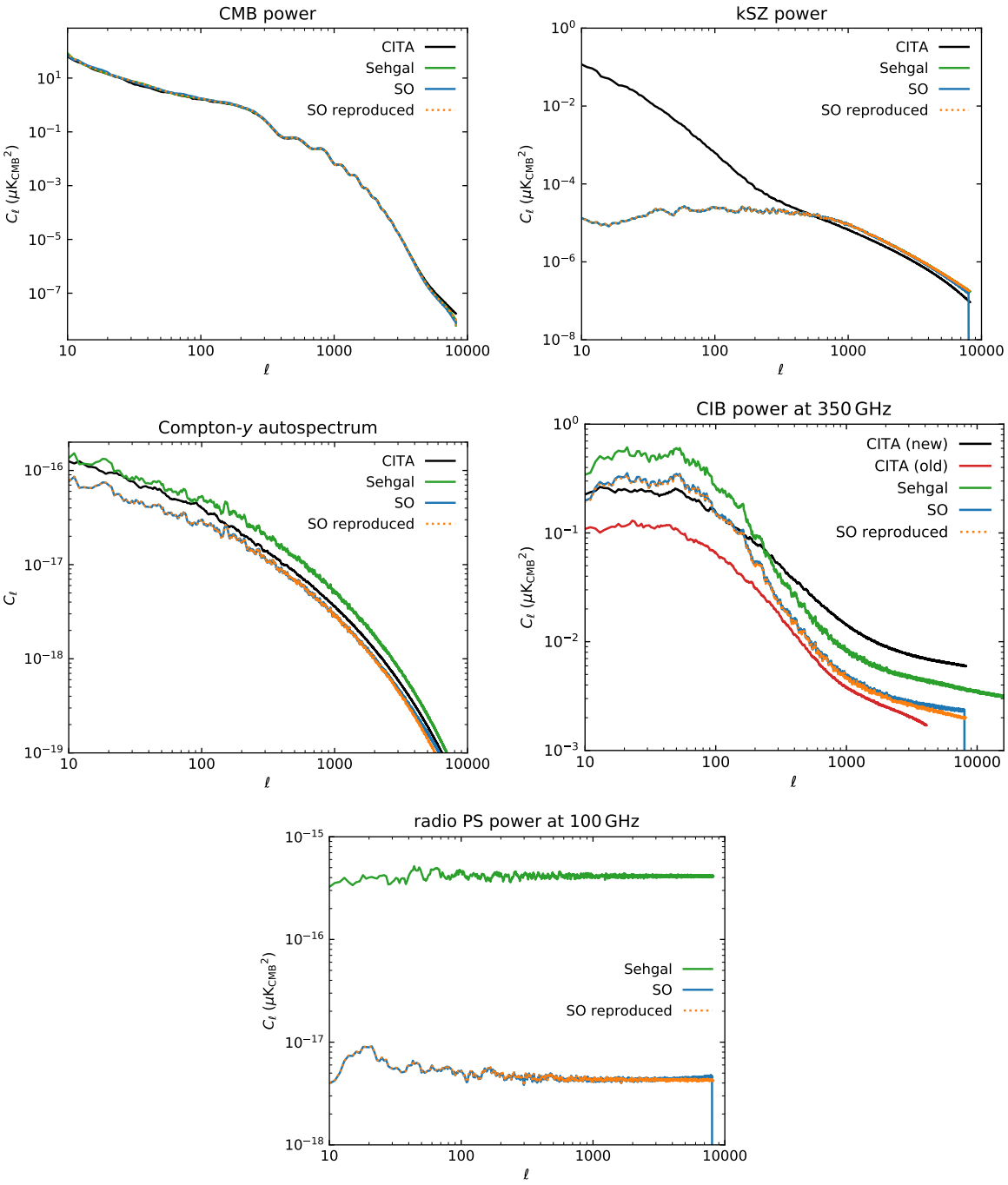

Figure 6 – Comparison of the power spectrum of the extragalactic microwave sky components.

References

Ade, P., Aguirre, J., Ahmed, Z., Aiola, S., Ali, A., Alonso, D. et al. The Simons Observatory: science goals and forecasts. *JCAP*, 2019:056, 2019. doi: 10.1088/1475-7516/2019/02/056.

Choi, S.K., Austermann, J., Basu, K., Battaglia, N., Bertoldi, F., Chung, D.T. et al. Sensitivity of the Prime-Cam Instrument on the CCAT-prime Telescope. *arXiv e-prints*, art. arXiv:1908.10451, 2019.

Erler, J., Basu, K., Chluba, J. and Bertoldi, F. Planck's view on the spectrum of the Sunyaev-Zeldovich effect. *MNRAS*, 476:3360–3381, 2018. doi: 10.1093/mnras/sty327.

Ferraro, S. and Hill, J.C. Bias to cmb lensing reconstruction from temperature anisotropies due to large-scale galaxy motions. *Physical Review D*, 97(2), 2018. ISSN 2470-0029. doi: 10.1103/physrevd.97.023512. URL http://dx.doi.org/10.1103/PhysRevD.97.023512.

George, E.M., Reichardt, C.L., Aird, K.A., Benson, B.A., Bleem, L.E., Carlstrom, J.E. et al. A measurement of secondary cosmic microwave background anisotropies from the 2500 square-degree spt-sz survey. *ApJ*, 799(2):177, 2015. ISSN 1538-4357. doi: 10.1088/0004-637x/799/2/177. URL http://dx.doi.org/10.1088/0004-637X/799/2/177.

Haslam, C.G.T., Klein, U., Salter, C.J., Stoffel, H., Wilson, W.E., Cleary, M.N. et al. A 408 MHz all-sky continuum survey. I - Observations at southern declinations and for the North Polar region. *A&A*, 100:209–219, 1981.

Haslam, C.G.T., Salter, C.J., Stoffel, H. and Wilson, W.E. A 408 MHz all-sky continuum survey. II. The atlas of contour maps. *Astronomy and Astrophysics Supplement Series*, 47:1–143, 1982.

Komatsu, E., Dunkley, J., Nolta, M.R., Bennett, C.L., Gold, B., Hinshaw, G. et al. Five-yearwilkinson microwave anisotropy probeobservations: Cosmological interpretation. *ApJ Supplement Series*, 180(2):330–376, 2009. ISSN 1538-4365. doi: 10.1088/0067-0049/180/2/330. URL http://dx.doi.org/10.1088/0067-0049/180/2/330.

Miville-Deschênes, M.A., Lagache, G., Boulanger, F. and Puget, J.L. Statistical properties of dust far-infrared emission. *A&A*, 469:595–605, 2007. doi: 10.1051/0004-6361:20066962.

Planck Collaboration. Planck 2015 results. X. Diffuse component separation: Foreground maps. *A&A*, 594:A10, 2016. doi: 10.1051/0004-6361/201525967.

Planck Collaboration, N., Arnaud, M., Ashdown, M., Aumont, J., Baccigalupi, C., Banday, A.J. et al. Planck2015 results. *A&A*, 594:A22, 2016h. ISSN 1432-0746. doi: 10.1051/0004-6361/201525826. URL http://dx.doi.org/10.1051/0004-6361/201525826.

Planck Collaboration, P.A.R., Aghanim, N., Armitage-Caplan, C., Arnaud, M., Ashdown, M., Atrio-Barandela, F. et al. Planck2013 results. xxi. power spectrum and high-order statistics

of theplanckall-sky compton parameter map. *A&A*, 571:A21, 2014d. ISSN 1432-0746. doi: 10.1051/0004-6361/201321522. URL http://dx.doi.org/10.1051/0004-6361/201321522.

Remazeilles, M., Dickinson, C., Banday, A.J., Bigot-Sazy, M.A. and Ghosh, T. An improved source-subtracted and destriped 408-MHz all-sky map. *MNRAS*, 451:4311–4327, 2015. doi: 10.1093/mnras/stv1274.

Sehgal, N., Bode, P., Das, S., Hernandez- Monteagudo, C., Huffenberger, K., Lin, Y.T. et al. Simulations of the Microwave Sky. *ApJ*, 709:920–936, 2010. doi: 10.1088/0004-637X/709/2/920.

Singh, S., Mandelbaum, R. and Brownstein, J.R. Cross-correlatingplanckcmb lensing with sdss: lensing–lensing and galaxy–lensing cross-correlations. *MNRAS*, 464(2):2120–2138, 2016. ISSN 1365-2966. doi: 10.1093/mnras/stw2482. URL http://dx.doi.org/10.1093/mnras/stw2482.

Stein, G., Alvarez, M.A. and Bond, J.R. The mass-Peak Patch algorithm for fast generation of deep all-sky dark matter halo catalogues and its N-body validation. *MNRAS*, 483(2):2236–2250, 2019. doi: 10.1093/mnras/sty3226.

Stein, G., Alvarez, M.A., Bond, J.R., van Engelen, A. and Battaglia, N. The Websky Extragalactic CMB Simulations. *arXiv e-prints*, art. arXiv:2001.08787, 2020.

Thorne, B., Dunkley, J., Alonso, D. and Næss, S. The Python Sky Model: software for simulating the Galactic microwave sky. *MNRAS*, 469:2821–2833, 2017. doi: 10.1093/mnras/stx949.